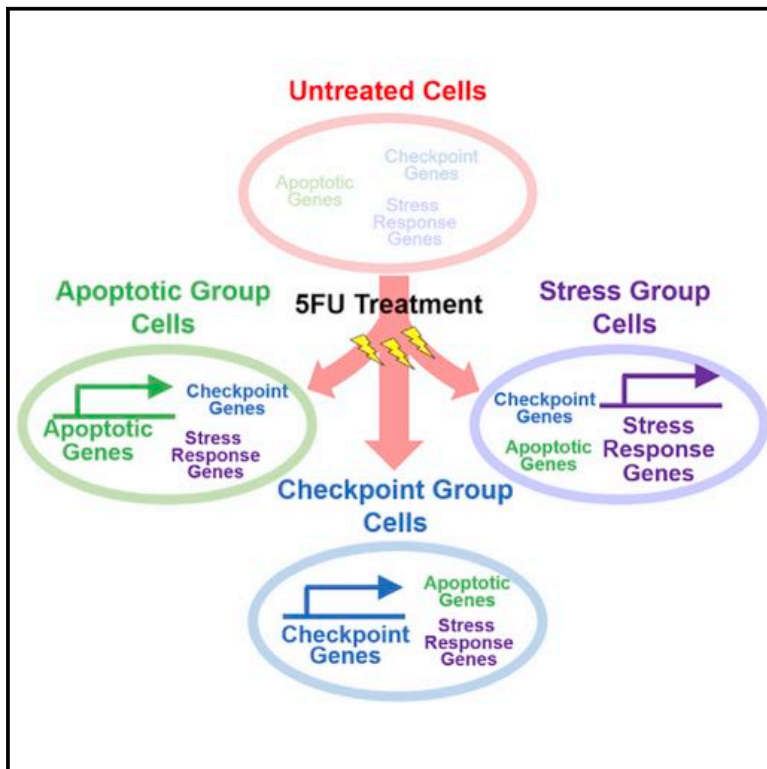


Cell Reports

Single-Cell Transcriptome Analysis of Colon Cancer Cell Response to 5-Fluorouracil-Induced DNA Damage

Graphical Abstract



Authors

Sung Rye Park, Sim Namkoong, Leon Friesen, ..., Hojoong Kwak, Hyun Min Kang, Jun Hee Lee

Correspondence

hmkang@umich.edu (H.M.K.),
leeju@umich.edu (J.H.L.)

In Brief

Park et al. characterize transcriptome responses of colon cancer cells to 5FU-induced DNA damage at single-cell resolution. Many DNA damage response genes are heterogeneously expressed across the cell population. Specifically, cells undergoing different fates had distinct transcriptomic landscapes, characterized by the expression of fate-specific DNA damage response genes.

Highlights

- Single-cell transcriptome responses to 5FU-induced DNA damage are characterized
- Transcriptome phenotypes underlying heterogeneous 5FU responses are identified
- Cell-fate-specific gene expression patterns after 5FU treatment are shown
- Key observations are reproduced in flow cytometry and other DNA damage treatments



Resource

Single-Cell Transcriptome Analysis of Colon Cancer Cell Response to 5-Fluorouracil-Induced DNA Damage

Sung Rye Park,^{1,2} Sim Namkoong,^{1,2,3} Leon Friesen,⁴ Chun-Seok Cho,¹ Zac Zezhi Zhang,² Yu-Chih Chen,^{5,6} Euisik Yoon,^{5,7,8} Chang H. Kim,⁴ Hojoong Kwak,⁹ Hyun Min Kang,^{2,*} and Jun Hee Lee^{1,10,*}

¹Department of Molecular & Integrative Physiology and Institute for Gerontology, University of Michigan Medical School, Ann Arbor, MI 48109, USA

²Department of Biostatistics and Center for Statistical Genetics, University of Michigan School of Public Health, Ann Arbor, MI 48109, USA

³Department of Biochemistry, College of Natural Sciences, Kangwon National University, Chuncheon, Gangwon 24341, Republic of Korea

⁴Department of Pathology and Mary H. Weiser Food Allergy Center, University of Michigan Medical School, Ann Arbor, MI 48109, USA

⁵Department of Electrical Engineering and Computer Science, University of Michigan College of Engineering, Ann Arbor, MI 48109, USA

⁶Forbes Institute for Cancer Discovery, University of Michigan, Ann Arbor, MI 48109, USA

⁷Department of Biomedical Engineering, University of Michigan College of Engineering, Ann Arbor, MI 48109, USA

⁸Center for Nanomedicine, Institute for Basic Science (IBS), and Graduate Program of Nano Biomedical Engineering (Nano BME), Advanced Science Institute, Yonsei University, Seoul 03722, Republic of Korea

⁹Department of Molecular Biology and Genetics, Cornell University, Ithaca, NY 14853, USA

¹⁰Lead Contact

*Correspondence: hmkang@umich.edu (H.M.K.), leeju@umich.edu (J.H.L.)

<https://doi.org/10.1016/j.celrep.2020.108077>

SUMMARY

DNA damage often induces heterogeneous cell-fate responses, such as cell-cycle arrest and apoptosis. Through single-cell RNA sequencing (scRNA-seq), we characterize the transcriptome response of cultured colon cancer cell lines to 5-fluorouracil (5FU)-induced DNA damage. After 5FU treatment, a single population of colon cancer cells adopts three distinct transcriptome phenotypes, which correspond to diversified cell-fate responses: apoptosis, cell-cycle checkpoint, and stress resistance. Although some genes are regulated uniformly across all groups of cells, many genes showed group-specific expression patterns mediating DNA damage responses specific to the corresponding cell fate. Some of these observations are reproduced at the protein level by flow cytometry and are replicated in cells treated with other 5FU-unrelated genotoxic drugs, camptothecin and etoposide. This work provides a resource for understanding heterogeneous DNA damage responses involving fractional killing and chemoresistance, which are among the major challenges in current cancer chemotherapy.

INTRODUCTION

Genotoxic chemotherapy is one of the most widely used anti-cancer treatments that utilize the sensitivity of cancer cells to DNA-damage-induced cell death. DNA damage can induce heterogeneous cell-fate responses, such as apoptosis, cell-cycle arrest, and chemoresistant survival. These heterogeneous fate responses are often the basis of fractional cell killing and tumor recurrence, which have been among the most significant challenges in cancer treatment.

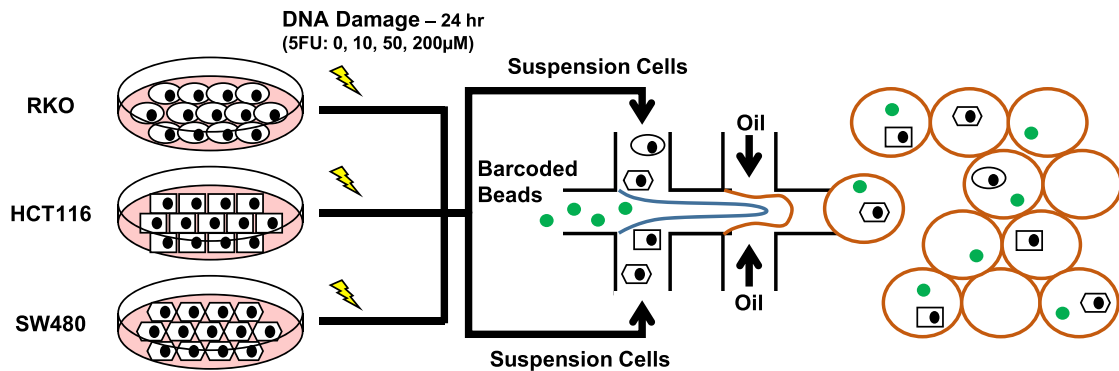
Through extensive studies, many molecular sensors, pathways, and mediators of the DNA damage response have been characterized (Harper and Elledge, 2007; Jackson and Bartek, 2009). Since the cell fates of individual cells after DNA damage are distinct from each other, the DNA damage response is now being characterized at the single-cell level by using live-cell reporters monitoring the status of DNA-damage-responsive components. These studies showed that longitudinal patterns of p53 (Hafner et al., 2019; Paek et al., 2016) or p21/CDKN1A expression (Barr et al., 2017; Hsu et al., 2019) are heterogeneous across

the population and serve as good indicators for cell fate after genotoxic injury. These findings also suggested that cells undergoing different fate responses may adopt distinct types of gene expression programs. Since distinct fate responses would require regulation of many genes, it is necessary to systematically profile single-cell transcriptomes, which could lead to a better understanding of the molecular heterogeneity in DNA damage responses.

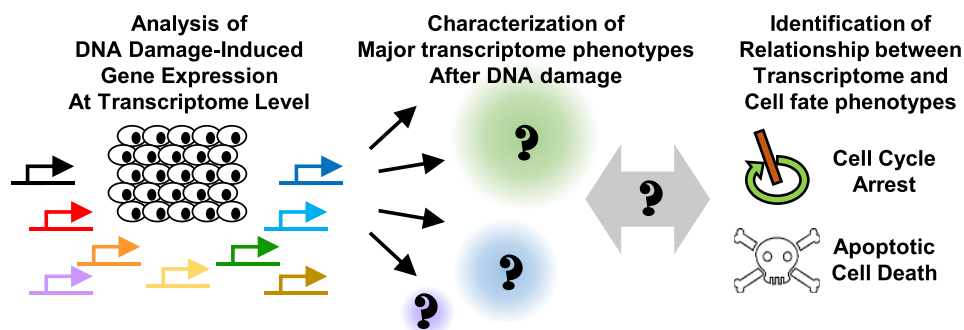
Colon cancer is the third most common cancer worldwide, and it is often treated with genotoxic chemotherapy using 5-fluorouracil (5FU) (Kuipers et al., 2015). Accordingly, 5FU treatment in colon cancer cell lines has been often used to investigate the cancer cell response to DNA damage (Bunz et al., 1999). Particularly, how cells alter their transcriptome in response to 5FU-induced DNA damage has been extensively characterized in this system (Chang et al., 2014; Kho et al., 2004; Sánchez et al., 2014; Wei et al., 2006). Using this cell-culture model of colon cancer chemotherapy, we characterized the individual cell response to genotoxic 5FU treatments using single-cell RNA sequencing (scRNA-seq) technology (Figure 1A). By analyzing



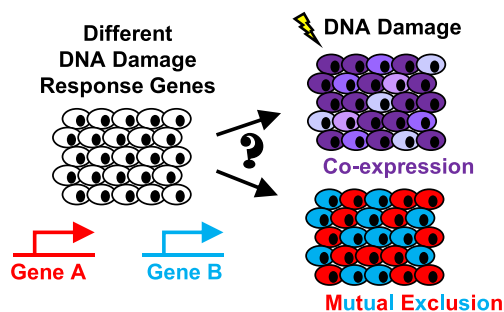
A Drop-seq combined with Genetic Multiplexing



B Analysis of Single Cell DNA Damage Response



C Characterization of Single Cell Gene Expression Pattern



D

Validation & Follow-up Through Flow Cytometry

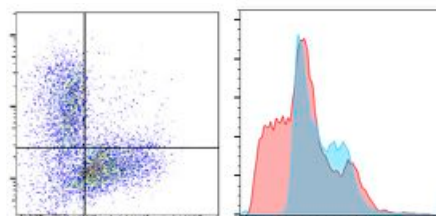


Figure 1. Resource Overview

(A) RKO, HCT116, and SW480 cells were 5FU treated and subjected to Drop-seq.

(B) DNA damage responses were characterized at the single-cell transcriptome level (left). Major transcriptome phenotypes were identified (center), and the relationships between these phenotypes and cell-fate outputs were investigated (right).

(C) The correlations between DNA-damage-induced expression patterns of individual genes were investigated. A hypothetical pair of two genes (gene A and gene B) may be co-expressed (upper path) or expressed in a mutually exclusive pattern (lower path) across single cells.

(D) Major findings from the scRNA-seq data were followed up by flow cytometry.

See also [Figure S1](#).

DNA-damage-induced gene expression at the transcriptome level, we were able to identify major transcriptome phenotypes after DNA damage and relate them to DNA-damage-induced cell-fate responses that include apoptosis and cell-cycle checkpoint ([Figure 1B](#)). We also identified that, in the single-cell population, two different DNA-damage-induced genes could be either co-expressed or expressed in a mutually exclusive pattern ([Fig-](#)

[ure 1C](#)). Finally, using flow cytometry experiments, we assessed whether the single-cell transcriptomic features could faithfully reflect the patterns of single-cell protein expression and cell-fate responses ([Figure 1D](#)). Collectively, this work paints a comprehensive picture of distinct single-cell transcriptomic profiles that closely reflect the heterogeneous cell-fate responses after DNA damage.

RESULTS

scRNA-seq Profiling Precisely Captures Cell-Line Identity and DNA Damage Response

For this study, we used RKO, HCT116, and SW480 cells, which are among the most frequently used colon cancer cell lines and represent distinct oncogenic features with respect to genetic mutations and genomic instability (Ahmed et al., 2013). As illustrated in Figure 1A, we treated these cell lines with 5FU. Some of the mRNAs highly induced by DNA damage—such as *CDKN1A*, which mediates p53-dependent cell-cycle arrest—were accompanied by strong upregulation of the corresponding protein levels at 24 h after 5FU treatment (Figure S1A).

Untreated or 5FU-treated cell lines were pooled and subjected to Drop-seq (Macosko et al., 2015; Figure 1A). We performed Drop-seq in 10 independent experiments with different combinations of 5FU-treated and untreated cells (Figure S1B). After a series of quality control processes (Figures S1C and S1D), each barcoded droplet was de-multiplexed using the genetic information captured in mRNA sequences (Kang et al., 2018), as described in STAR Methods. A total of 10,421 single-cell transcriptome profiles were determined from untreated and 5FU-treated RKO (3,053 cells), HCT116 (2,699 cells), and SW480 (4,669 cells) cell lines (Figure S1E). These cell lines exhibited distinct transcriptomic profiles, as visualized by principal component analysis (PCA), t-distributed stochastic neighbor embedding (t-SNE), and uniform manifold approximation and projection (UMAP) (Figure S1F; Becht et al., 2018; van der Maaten and Hinton, 2008).

For all three cell lines in t-SNE and UMAP manifolds, 5FU-treated cells were clustered in locations that were distinct from untreated cells (Figure S1G), indicating that the 5FU-induced DNA damage substantially altered the single-cell transcriptomes of these cell lines.

Expression of classical DNA damage response genes, such as *CDKN1A*, *MDM2*, and *GADD45A*, which are targets of the tumor suppressor p53, were pronouncedly upregulated after 5FU treatment in p53-wild-type RKO and HCT116 cells but not so strongly in p53-mutated SW480 cells (Figure S1H). However, 5FU induction of these genes was statistically significant in all cell lines examined (Figure S1H). Likewise, *CCNB1*, *CDKN3*, and *CDC20*, mitosis-controlling genes that are downregulated after 5FU stress (Kho et al., 2004), were strongly reduced in RKO and HCT116 cells but less so in SW480 cells (Figure S1I). In contrast, DNA-damage-dependent regulation of some genes, such as *MAP1LC3B* (upregulated), *RPL10A*, and *RPL27A* (downregulated), was robustly observed in all three cell lines (Figure S1J).

5FU Treatment Induces Three Distinct Cell Groups with Unique Transcriptome Landscapes

We initially focused on RKO cells, which exhibited the most pronounced DNA damage response in our dataset (Figures S1H–S1J). First, we explored the heterogeneity of single-cell transcriptome profiles with high-dimensional clustering. We identified four major clusters (untreated, apoptotic, checkpoint, and stress; or U, A, C, and S, respectively, as shown in Figures 2A and 2B), where one cluster (untreated; $n = 1,597$) mainly con-

sists of untreated cells, while the other three clusters (apoptotic, checkpoint, and stress; $n = 800, 571, \text{ and } 85$, respectively) correspond to 5FU-treated cells (Figures 2C and 2D). These clusters were manifested in both t-SNE (Figure 2A) and UMAP (Figure 2B) manifolds, as well as PCA (Figure 2E). Even a single batch of cells exhibited the heterogeneity that corresponds to each of these clusters (Figures S2A–S2D), indicating that the heterogeneous response of DNA damage is observed across different doses or batches of DNA damage treatment.

To infer biological characteristics relevant to each cluster, we isolated the top 30 upregulated genes for each through differential expression analysis based on the non-parametric Wilcoxon rank-sum test (Figure S2E; Table S1). Using the list of cluster-specific top markers, we performed gene enrichment analysis using the Gene Ontology database of biological pathways (GO-BP) (Gene Ontology Consortium, 2015). Only 21 genes were significantly upregulated in the cluster with untreated cells (adjusted $p < 0.05$), and this gene list showed a weak enrichment of genes with various housekeeping functions (adjusted $p \approx 0.01$; Figure 2F). This cluster with untreated cells was named the untreated group (or U, as shown in Figure 2G). In contrast, 5FU-treated clusters exhibited much stronger enrichment of genes involved in various DNA damage response processes (adjusted $p < 0.0001$; Figure 2F). The largest 5FU-treated cluster was highly enriched with genes involved in the apoptotic pathway (Figure 2F); therefore, we named this group the apoptotic group (or A, as shown in Figure 2G), according to its presumed biological characteristics. In contrast, the second largest 5FU-treated cluster was enriched with DNA-damage-induced cell-cycle checkpoint genes (Figure 2F); therefore, we named this group the checkpoint group (or C, as shown in Figure 2G). The smallest cluster was enriched with stress response genes (Figure 2F) and was named the stress group (or S, as shown in Figure 2G).

We also found that proportions across groups were substantially changed according to the dose of 5FU treatment (Figures S2A–S2D). Although checkpoint group cells were abundantly found across all doses of 5FU treatment, apoptotic group cells were only abundant in cells treated with 10 and 50 μM 5FU and rarely found in cells treated with 200 μM 5FU (Figures S2A–S2D). It is possible that high levels of DNA damage by 200 μM 5FU accelerated the apoptotic progression of apoptotic group cells, facilitating apoptosis-associated RNA decay (Thomas et al., 2015), which will render the population undetectable from the scRNA-seq dataset. In contrast to the apoptotic group, the numbers of cells in the checkpoint and stress groups were not reduced at the high 5FU dose (Figures S2B–S2D), indicating that the cells in these groups were relatively resistant to the genotoxic stress induced by 5FU.

Another interesting observation is that, in the apoptotic and checkpoint groups of cells, dose-dependent subclusters were identified in both t-SNE and UMAP manifolds (Figures 2C and 2D); the apoptotic group has two subclusters corresponding to 10 and 50 μM 5FU treatments, and the checkpoint group has three subclusters corresponding to 10, 50, and 200 μM 5FU treatments (Figures 2C and 2D). Since granulation of the dose-dependent subclusters was coherently observed across the different experimental batches (Figure S2A), these subclusters

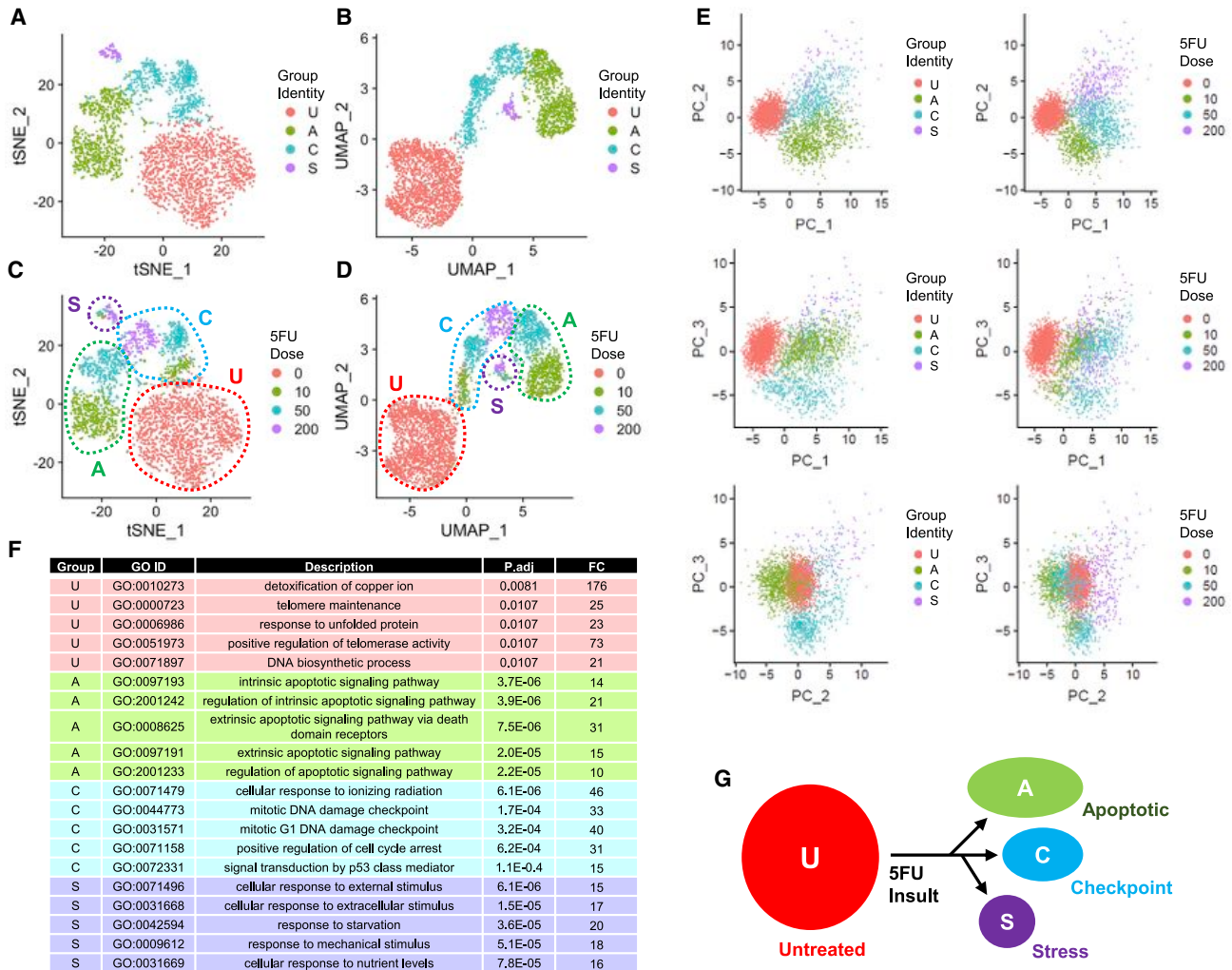


Figure 2. 5FU Treatment Induces Three Distinct Types of Single-Cell Transcriptome Responses

(A–D) t-SNE and UMAP manifolds colored with group identity (A and B) and 5FU dose (C and D).

(E) PCA manifold of RKO cells colored with group identity (left) and 5FU dose (right).

(F) GO-BP enrichment analysis of the top 30 markers for each group. Top 5 GO-BP terms, ordered by adjusted p values (P.adj), are summarized in the table. FC, fold enrichment.

(G) A schematic model depicting 5FU-induced transcriptomic responses of RKO cells.

See also [Figure S2](#) and [Table S1](#).

are likely to represent dose-dependent biological variations in the transcriptional responses to DNA damage.

Different 5FU-Induced Cell Groups Exhibit Distinct Patterns of p53 Target Gene Expression

Interestingly, when the pathway enrichment analysis was performed using the Kyoto Encyclopedia of Genes and Genomes (KEGG) database ([Kanehisa and Goto, 2000](#)), all 5FU-treated groups identified the p53 signaling pathway as the top pathway enriched in each group ([Figure 3A](#)). Further inspection showed that more than half of the marker genes specific to the apoptotic or checkpoint groups are associated with the p53 pathway ([Figure 3A](#), gene counts are given in parentheses; [Figures 3B–3D](#), gene lists). Intriguingly, a vast majority (93%) of these marker

genes were exclusively found in a single group, and even the remaining three genes (*MDM2*, *GADD45A*, and *RRM2B*; 7%) were found only in two groups but not in the third ([Figures 3B–3D](#)). For instance, *MDM2*, a negative-feedback regulator of p53, was highly expressed in the checkpoint and stress groups but less so in the apoptotic group ([Figures 3C and 3D](#), pink boxes). In contrast, *ISG15*, a recently identified positive-feedback regulator of p53 ([Park et al., 2016](#)), was upregulated only in the apoptotic group but not in the checkpoint or stress group ([Figure 3B](#), yellow box).

Based on these preliminary observations, we performed a more thorough analysis of p53 target gene transcription, using a recently assembled list of p53 target genes in the human genome ([Fischer, 2017](#)). From this list, we found that most of

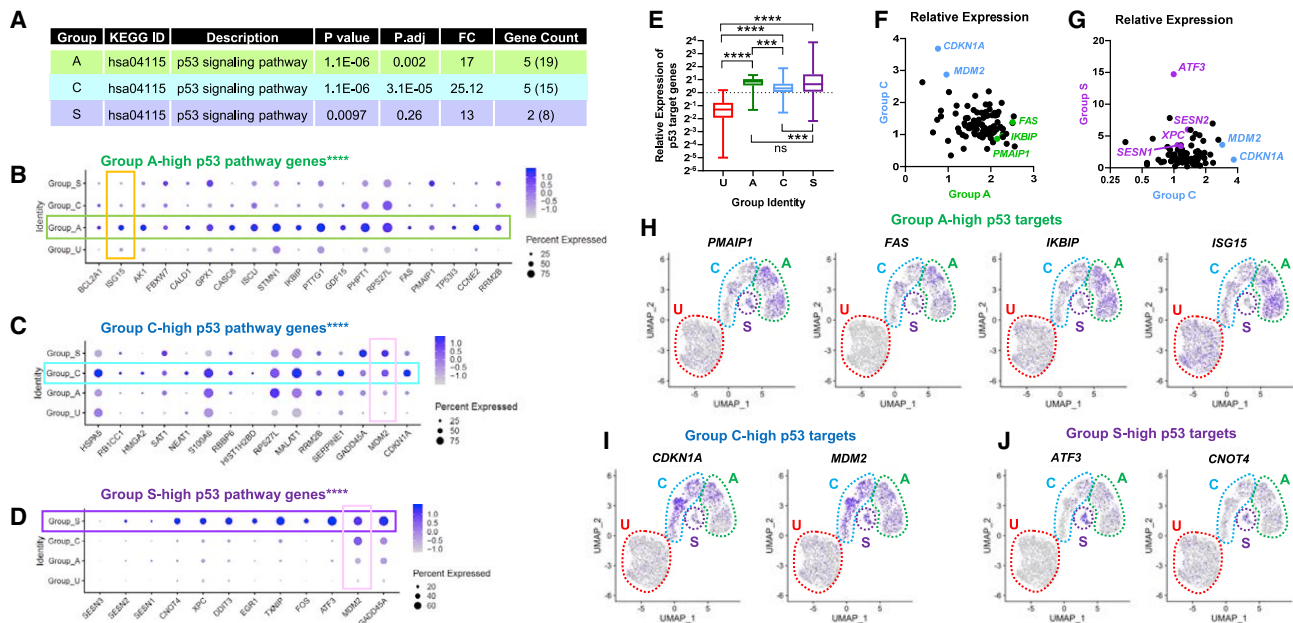


Figure 3. Diversified Patterns of p53 Target Gene Expression after DNA Damage

(A) Pathway enrichment analysis using the KEGG database. Counts in parentheses include genes whose involvement in p53 pathway was documented in the literature but was not included in the KEGG database. P.adj, adjusted p value; FC, fold enrichment.

(B–D) Dot plot of the p53 pathway genes that were in the top 30 markers for each group. The size of the dot reflects the percentage of cells expressing the markers, while the color encodes average expression levels across all cells within the group (blue indicates high). *CNOT4* and *SESNs* were not in the top 30 markers but were among the genes upregulated in the stress group.

(E–G) Average expression levels of individual p53 target genes in each group, normalized by their averaged expression in all cells, are presented in boxplot (E) and correlation scatterplots (F and G). The list of p53 target genes was obtained from a recent review (Fischer, 2017). Among the 116 targets, 89 were detected in our dataset and used for this analysis. Each dot in the scatterplots represents an individual p53 target gene. *** $p < 0.001$; **** $p < 0.0001$; ns, non-significant, in Tukey's multiple comparison test.

(H–J) Gene expression feature plots of representative group-specific marker genes. Approximate boundaries for each group are indicated by a dotted line. See also Figure S3.

the p53 targets were induced in all three 5FU-treated groups compared to the untreated group (Figure 3E) and that their induction was generally higher in the apoptotic and stress groups than in the checkpoint group (Figure 3E). However, the checkpoint group exhibited the strongest expression of *CDKN1A* and *MDM2* (Figures 3F and 3G). The pro-apoptotic p53 target genes such as *PMAIP1*, *FAS*, and *IKBIP* (Figure 3F) and p53 target genes important for stress resistance such as *ATF3*, *XPC*, and *SESNs* (Figure 3G), were the most highly expressed in the apoptotic and stress groups, respectively. Group-specific expressions of these group-specific p53 target genes were also manifested in the gene expression feature plots (Figures 3H–3J).

We processed our scRNA-seq data through Markov affinity-based graph imputation of cells (MAGIC) (van Dijk et al., 2018) and observed clearer patterns in the group-specific gene expression distributions (Figures S3A–S3C), compared to the results before imputation that suffer information sparsity and technical noise (Figures S3D–S3F). Using the imputed expressions, we examined how different p53 pathway genes were co-expressed in different cell populations. Scatterplots of imputed data clearly show that different cell groups exhibited different patterns of p53 target gene expression after 5FU treatment (Fig-

ure 4A). The analyses indicated that the 5FU dose also affected the single-cell expression of these genes (Figure 4B).

To further characterize the effects of dose and group on p53 target gene expression, we performed a granular analysis of dose-dependent subclusters in each group of cells. Apoptotic-group-specific *PMAIP1* and *FAS* genes, as well as checkpoint-group-specific *CDKN1A* and *MDM2* genes, were more strongly expressed when the cells were treated with 50 μ M 5FU, compared to the cells treated with 10 μ M 5FU (Figures 4C and 4D). These genes were also more strongly expressed in their corresponding groups of cells (Figures 4C and 4D). The effects of dose and group identity, as well as the synergistic interaction between them, showed strong statistical significance ($p < 0.0001$, two-way ANOVA). However, interestingly, when the cells were treated with 200 μ M 5FU, apoptotic group cells were not observed (Figures S2B–S2D), and checkpoint group cells showed reduced expression levels of all of these four genes (Figures 4C and 4D). Stress-group-specific *ATF3* and *DDIT3* genes were highly expressed in stress group cells, compared to those in apoptotic or checkpoint group cells (Figure 4E). These results demonstrate that cells exhibit heterogeneous patterns of p53 target gene expression, which might be associated with distinct fate responses (Figure 4F).

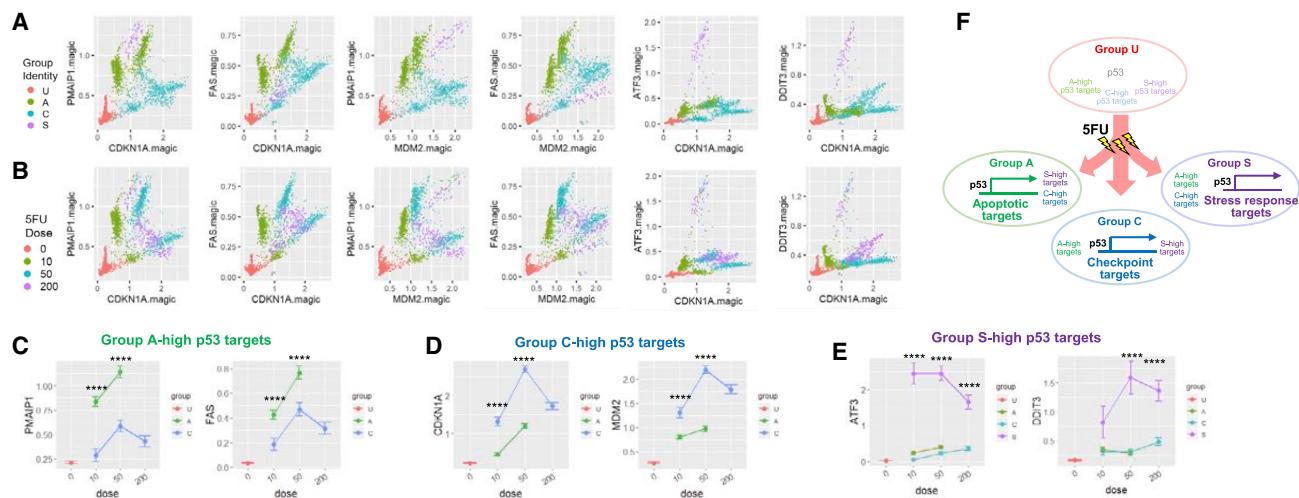


Figure 4. Single-Cell Heterogeneity in p53 Target Gene Expression after DNA Damage

(A and B) Scatterplots of indicated gene expression in single cells, imputed through *magic*. Each dot represents an individual cell indicated in color according to its group identity (A) or 5FU dose (B).

(C–E) Analyses of p53 target gene expression (y axis) across different subgroups of cells partitioned with 5FU dose (x axis) and group identity (color). Untreated, apoptotic, and checkpoint groups were analyzed. Because the stress group contained a very small number of cells ($n < 50$), it was only analyzed for stress group-specific markers (E), which produced statistically interpretable results. Data are presented as mean \pm SEM. **** $p < 0.0001$, in Sidak's multiple comparison test between the apoptotic and checkpoint groups (C and D) or between the stress group and all the other groups (E).

(F) Schematic model depicting the group-specific expression of p53 target genes.

See also Figure S4.

Apoptotic and Checkpoint Groups Exhibit Distinct Cell-Cycle Characteristics

From the scRNA-seq dataset, we estimated the stage of the cell cycle for each cell by analyzing the expression of cell-cycle-specific genes (Nestorowa et al., 2016; Tirosh et al., 2016). The analysis suggested that the checkpoint group, as expected, had a higher number of non-cycling cells (expressed as G1), compared to the other groups (Figures S4A and S4B). In contrast, the cells of the apoptotic group highly expressed several S and G2/M marker genes, such as *CCNE2*, *CDK1*, and *PCNA* (Figure S4C). The expression of these genes in the apoptotic group was even significantly higher than that in the untreated group (Figure S4C; $p < 0.0001$ for all genes and doses). However, other classical markers of cell-cycle progression such as minichromosome maintenance (MCM) (G1 to S progression), as well as cyclin B and Aurora kinase genes (G2 to M progression), were downregulated in the apoptotic group, compared to the untreated group (Figure S4D). These results suggest that the apoptotic group is not in a normal cell-cycling state, while the checkpoint group is in a classical cell-cycle arrest. However, as the cell-cycle estimation from the scRNA-seq data is through a speculative algorithm (Nestorowa et al., 2016; Tirosh et al., 2016), we further investigated how different single-cell transcriptome groups are associated with specific cell-fate responses after the 5FU treatment.

Flow Cytometry Confirms Heterogeneous DNA Damage Response at the Protein Level

CCNE2 and *CDKN1A* are among the top differentially regulated genes distinguishing the apoptotic and checkpoint groups (Table S1). Scatterplot analysis using imputed expression demonstrated that, following 5FU treatment, most apoptotic group cells

showed a *CCNE2*-high and *CDKN1A*-low profile, while most checkpoint group cells exhibited a *CCNE2*-low and *CDKN1A*-high profile (Figure 5A). Stress group cells were located between the apoptotic and checkpoint groups but were very small in numbers. In contrast to the DNA-damage-treated cells, the untreated group cells appeared as a single tight cluster (Figure 5A).

To monitor *CCNE2* and *CDKN1A* protein expression across single cells, we performed flow cytometry. Untreated cells showed a single dense population of relatively low expression of the two protein markers (U in Figure 5B). 5FU treatment induced stronger expression of these markers; however, as observed from the scRNA-seq data (Figure 5A), the induction of *CCNE2* and *CDKN1A* was largely mutually exclusive, forming two distinct populations: *CCNE2*-high, *CDKN1A*-low apoptotic group cells (A in Figure 5B) and *CCNE2*-low, *CDKN1A*-high checkpoint group cells (C in Figure 5B). A similar separation of cell groups was observed with different doses of 5FU (Figure 5C). At the highest concentration (200 μ M), 5FU treatment induced significantly higher numbers of double-negative (*CCNE2*-low, *CDKN1A*-low) cells, which appeared to be dead cells after extensive DNA damage and apoptosis (Figure 5C).

The imputed scRNA-seq data indicate that *MDM2*, another checkpoint group marker, could also be used to distinguish the apoptotic and checkpoint groups (Figure 5D). Flow cytometry indeed identified the *CCNE2*-high, *MDM2*-low apoptotic group and the *CCNE2*-low, *MDM2*-high checkpoint group in 5FU-treated cells (Figure 5E).

We also tested whether these observations could be generalized to other types of genotoxic chemotherapy treatments beyond 5FU. Treatment with camptothecin and etoposide also induced the emergence of the *CCNE2*-high, *CDKN1A*-low apoptotic group

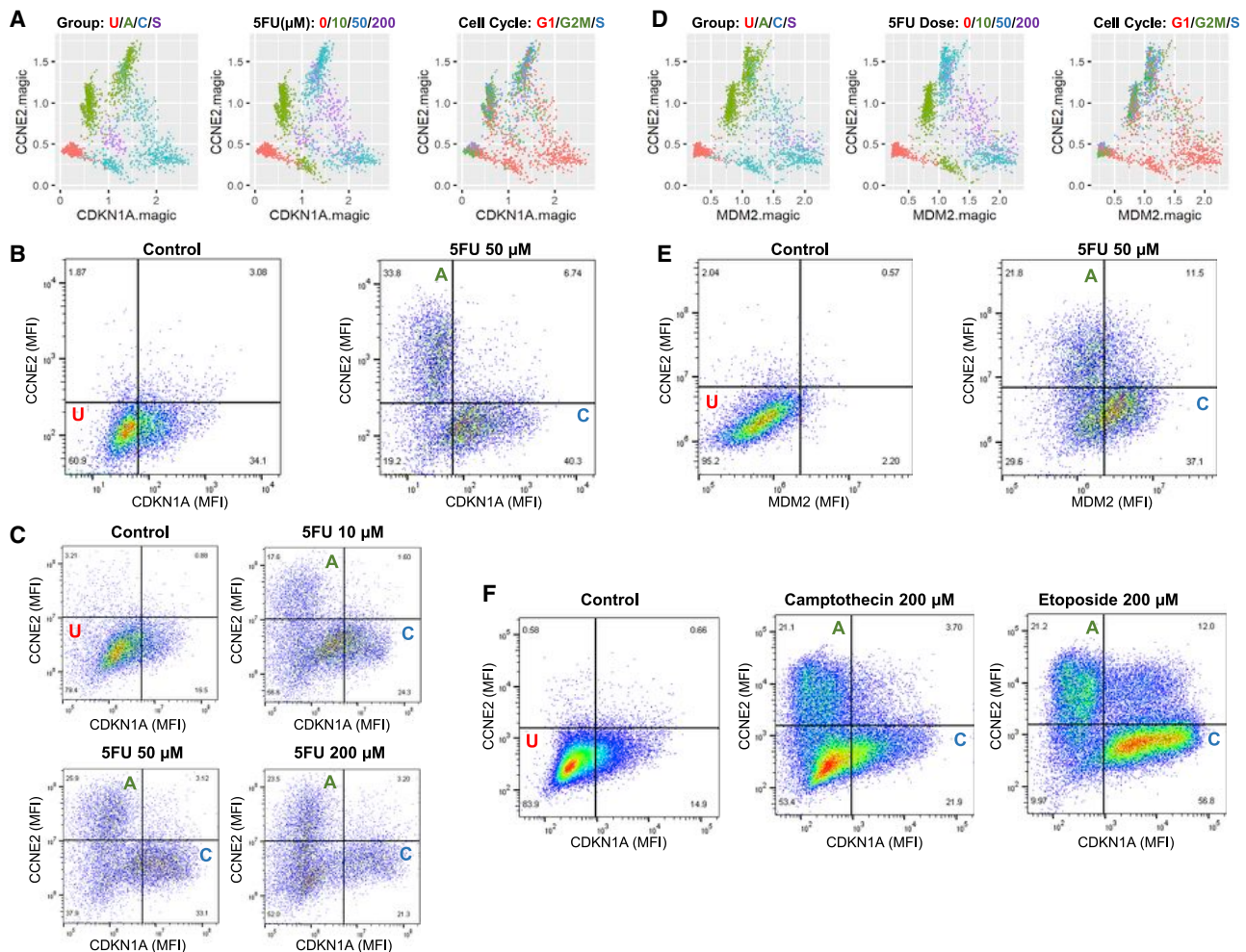


Figure 5. Heterogeneous mRNA and Protein Expression in DNA Damage Response

(A–F) In (A) and (D), scatterplots of indicated mRNA expression in single cells, imputed through *magic*. Each dot represents an individual cell colored with its group identity (left), 5FU dose (center), or estimated cell-cycle phase (right).

(B, C, E, and F) Flow cytometry dot plots showing indicated protein expression. Percent cells in each quadrant gate are indicated. MFI, mean fluorescence intensity.

See also [Figure S5](#).

and the CCNE2-low, CDKN1A-high checkpoint group (Figure 5F). Thus, the heterogeneous single-cell response to DNA damage appears to be conserved across different genotoxic drugs.

Cells in the Apoptotic Group Undergo Apoptosis

In forward scatter versus side scatter (FSC/SSC) analyses, cells in the checkpoint and apoptotic groups showed different characteristics. Compared to the checkpoint group cells, the apoptotic group cells had more variations in FSC values, which is indicative of variable cell size, while exhibiting somewhat lower SSC values, which is indicative of a decreased intracellular complexity (Figures S5A and S5B).

To further characterize the checkpoint group and apoptotic group cells, we performed the DNA content analysis. 5FU treatment induced a strong accumulation of a sub-G1 population, which is suggestive of cell death (Figure 6A). To perform

group-specific analysis, we partitioned the 5FU-treated cell population into the CCNE2-high, CDKN1A-low apoptotic group and the CCNE2-low, CDKN1A-high checkpoint group (Figure 6B, left) and analyzed their DNA contents separately (Figure 6B, right). Interestingly, roughly half of the apoptotic group cells appear as sub-G1 (blue in Figure 6B, right), indicating that the apoptotic group contained many dying cells. In contrast, the checkpoint group did not have sub-G1 cells, and most of the cells were assigned to the G1 phase with a minor population in the G2 phase (red in Figure 6B, right).

We also performed a converse analysis—we first gated the entire sub-G1 population from the 5FU-treated cells (Figure 6C, left) and analyzed the levels of CCNE2 and CDKN1A expression (Figure 6C, center). Most of the sub-G1 population was almost exclusively found in the apoptotic group but not in the checkpoint group (Figure 6C, center).

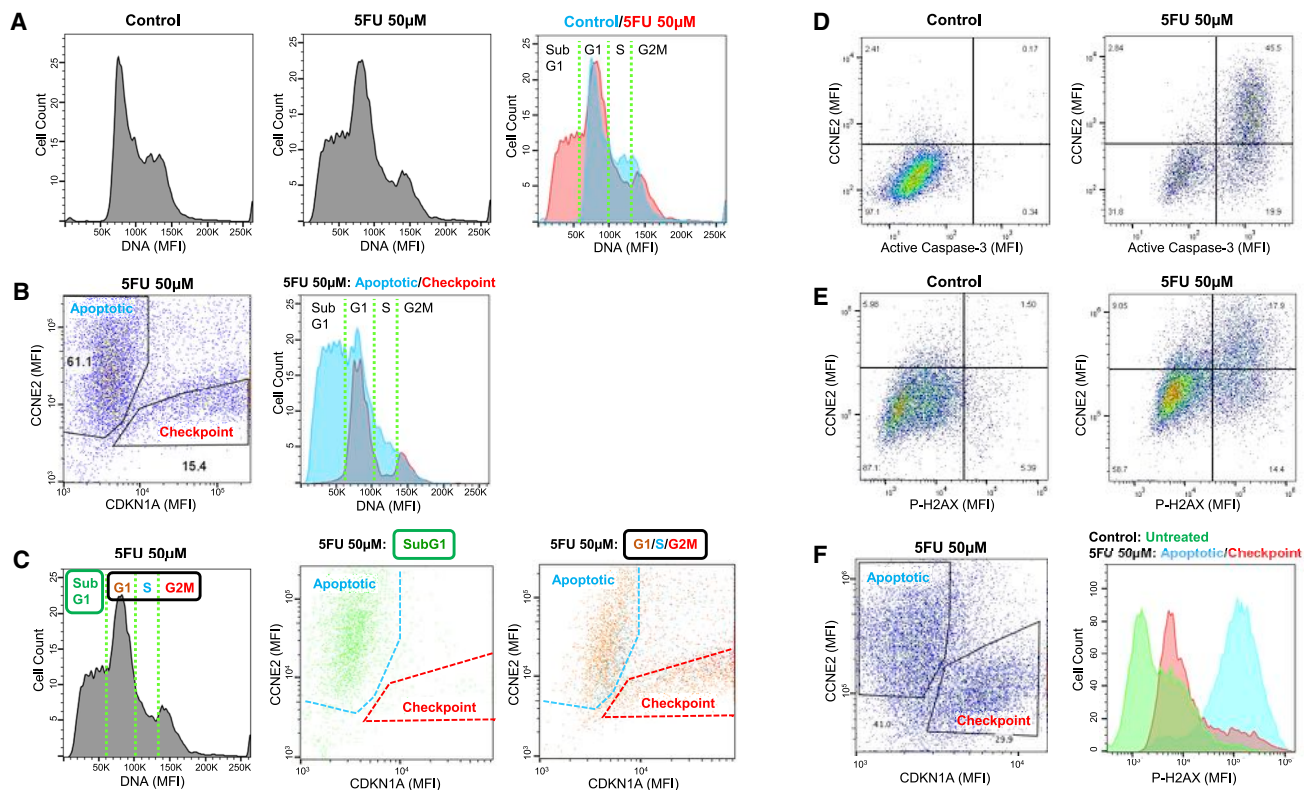


Figure 6. Flow Cytometry Verifies the Cell Fates of the Apoptotic and Checkpoint Groups

(A) DNA contents of control (left) and 5FU-treated (center) cells were compared with each other (right). Estimated cell-cycle stages were indicated by dotted green lines (right).

(B) From the 5FU-treated cells (center panel in A), cells in the apoptotic and checkpoint groups were separately analyzed for their DNA content. Gating scheme is shown in the left panel. The DNA content was separately analyzed for the gated apoptotic group (blue, right) or the checkpoint group (red, right).

(C) The whole 5FU-treated cells (left, same as center panel in A) were first gated on cell-cycle stages: sub-G1 (green; center) and G1/S/G2M (brown, blue, and red; right) cells and the subsets are indicated on the flow cytometry plots showing the expression of CCNE2 and CDKN1A.

(D and E) Flow cytometry analysis of indicated protein expression.

(F) From the 5FU-treated cells (right panel in E), cells in the apoptotic and checkpoint groups were separately analyzed for their P-H2AX expression. Gating scheme is shown in the left panel. P-H2AX expression by the cells of untreated (green), apoptotic (blue), and checkpoint (green) groups is indicated in the right panel.

MFI, mean fluorescence intensity. See also Figure S6.

Although almost half of the apoptotic group cells exhibited a sub-G1 DNA profile, many cells in the apoptotic group still had DNA contents greater than a diploid genome (Figures 6B and 6C). In addition, both apoptosis and necrosis can induce sub-G1 cells (Darzynkiewicz et al., 1997). Therefore, to examine whether the apoptotic group cells were, indeed, undergoing apoptotic cell death, we monitored caspase cascade activation, an authentic and specific marker of apoptosis (Srinivasan et al., 1998). Flow cytometry showed that most of the CCNE2-high apoptotic group cells expressed high levels of activated caspase-3 (Figure 6D). In contrast, CCNE2-low checkpoint group cells expressed relatively low levels of cleaved caspase-3 compared to the apoptotic group cells (Figure 6D). These results demonstrate that cells in the apoptotic group were, indeed, undergoing apoptosis.

Experiments using camptothecin and etoposide also produced results similar to the 5FU experiments. The apoptotic group cells exhibited a sub-G1 DNA profile, while the checkpoint

group cells showed a G1-arrested DNA profile (Figures S5C and S5D).

The Apoptotic Group Exhibits a Higher Level of DNA Damage than the Checkpoint Group

Through phosphorylated histone H2AX (P-H2AX), a quantitative marker for DNA damage (Sharma et al., 2012), we examined the levels of DNA damage in single cells. Although the level of P-H2AX was low in untreated control cells, CCNE2-low, CDKN1A-high checkpoint group cells showed a slightly increased level of P-H2AX staining (Figures 6E and 6F). In contrast, CCNE2-high, CDKN1A-low apoptotic group cells showed a much higher level of P-H2AX staining (Figures 6E and 6F), indicating more severe DNA damage in the apoptotic group cells. A higher level of DNA damage in the apoptotic group might have promoted the apoptotic fate determination. Also, caspase-activated DNases in the apoptotic cells (Enari et al., 1998) might have produced even more double-strand DNA

breaks. These results collectively confirm the presence of distinct biological cell fates following DNA damage and their relationship with *CCNE2* and *CDKN1A* expression patterns.

The Stress Group Is Characterized by Expression of Stress-Responsive Transcription Factors

The stress group is a small group of cells that were consistently observed throughout the different doses and batches of 5FU treatment. Stress group cells expressed high levels of stress-responsive transcription factors, including *ATF3* and *FOS*, as well as their targets (Figures S6A and S6B; Table S1). *SESN2*, a DNA-damage-inducible p53 target (Ho et al., 2016), was also highly expressed in the stress group but less so in the other groups (Figure 3D).

ATF3 and *FOS*, which are among the top stress-group-specific markers (Table S1), could be used to distinguish the stress group from the other groups in an imputed scRNA-seq dataset as the *ATF3/FOS*-high, *CDKN1A*-low group (Figures S6C and S6D). Flow cytometry with antibodies to *ATF3*, *FOS*, and *CDKN1A* identified such stress-group-like populations in the 5FU-treated cells (S in Figures S6E and S6F).

HCT116 Cells Exhibit 5FU-Induced Differentiation of Apoptotic and Checkpoint Groups

Finally, we evaluated whether the observations in the RKO cell line were reproduced in the HCT116 and SW480 cell lines. HCT116 and SW480 cells showed a clear dose response in altering the single-cell transcriptome profile after 5FU treatment (Figures 7A and 7C). However, they also showed very strong batch-dependent variations in the transcriptome (Figures 7B and 7D) that were not seen in the RKO dataset (Figure S2A). For instance, in the HCT116 dataset, the “0C” batch of untreated group cells produced a transcriptome cluster that is distinct from all the other batches (Figure 7B). Also, in the SW480 dataset, all batches were clustered in different locations in the UMAP manifold (Figure 7D). This strong batch effect made it difficult to perform a systematic analysis on the HCT116 and SW480 datasets as was performed on the RKO dataset.

Therefore, we instead tested whether the patterns of heterogeneous DNA damage response, initially observed from the RKO dataset, could be replicated in the HCT116 and SW480 datasets. We examined the expression of the RKO group-specific markers, such as *CCNE2*, *CDKN1A*, and *ATF3*, respectively representing the apoptotic, checkpoint, and stress groups. In the HCT116 dataset, we were able to identify two different groups of cells, apoptotic-like and checkpoint-like groups (A and C, respectively, in Figures 7E–7G), where *CCNE2* and *CDKN1A* expression was regulated in a diametrically opposite way. HCT116 differentiation into apoptotic-like and checkpoint-like groups was observed across all doses and experimental batches of 5FU treatment (Figure S7A). However, we were unable to find specific cell clusters that represent the *ATF3*-high stress-like group in the HCT116 dataset (Figure 7H). The apoptotic-like and checkpoint-like groups (A and C, respectively, in Figure 7I) in HCT116 not only showed contrasting expression patterns of *CCNE2* and *CDKN1A* but also differentially expressed other cell-cycle-regulating genes, such as *PCNA* and *CDK1* (Figure 7J). These results indicate that

HCT116 cells exhibit heterogeneous cell-cycle responses, as was observed in the RKO dataset.

Some Genes Are 5FU Regulated across All Heterogeneous Populations of Cells

In contrast to the RKO and HCT116 cells, *CCNE2* and *CDKN1A* did not show contrasting gene expression patterns in the SW480 dataset, although their expression was slightly elevated after 5FU treatments throughout the population (Figures 7K, 7L, and S7B). Likewise, *ATF3* expression was induced after 5FU treatment but did not show specific patterns of expression across the single-cell population (Figures 7M and S7B). Therefore, the heterogeneous transcriptome responses to 5FU, initially observed from the RKO dataset, do not seem to be well conserved in SW480 cells. Interestingly, some of the genes whose expression is strongly affected by 5FU treatment in the SW480 dataset, such as *MAP1LC3B*, *MAP1LC3B2*, *FKBP3*, and *RPL10A*, showed a similar dose-dependent regulation in the RKO and HCT116 datasets (Figures 7N–7P and S7C–S7E) and across all the groups undergoing distinct fate responses (Figures 7O and 7P). These results indicate that there are groups of genes that are commonly regulated by 5FU treatment across all heterogeneous populations of cells.

DISCUSSION

This study approached the heterogeneous DNA damage responses using scRNA-seq technology. We demonstrated that 5FU treatment induces three distinct transcriptome phenotypes that are each different from the untreated cell transcriptome in colon cancer cells. These distinct transcriptome phenotypes turned out to be associated with the major cell-fate responses to DNA damage, including apoptosis, cell-cycle arrest, and stress response. Many DNA damage response genes showed differential expression across the three cell groups, as summarized in the Results section and Table S1.

In addition to depositing all the raw and processed sequencing data into the Gene Expression Omnibus (GEO) repository (see STAR Methods for details), we also have made our dataset available to biological researchers through an interactive online resource (https://lee.lab.medicine.umich.edu/dna_damage), which has an intuitive graphical user interface for exploring our scRNA-seq dataset. Using this online tool, researchers can easily navigate the dataset, which has a vast amount of information. For instance, they can examine how individual genes are expressed across single cells before and after 5FU treatments and how the specific gene expression is correlated with the 5FU dose, group identity, batch identity, or single-cell expression of other genes. This online tool can also be used by researchers to test new hypotheses and generate new data; therefore, it has the potential to accelerate future research on DNA damage responses.

Although our dataset opens an avenue for exploring single-cell DNA damage responses, there are a few limitations that we should consider. First, our scRNA-seq dataset, by definition, only contains information on RNA levels, not protein levels. There is an inherent time delay between transcription and translation, which can reduce the concordance between mRNA and protein

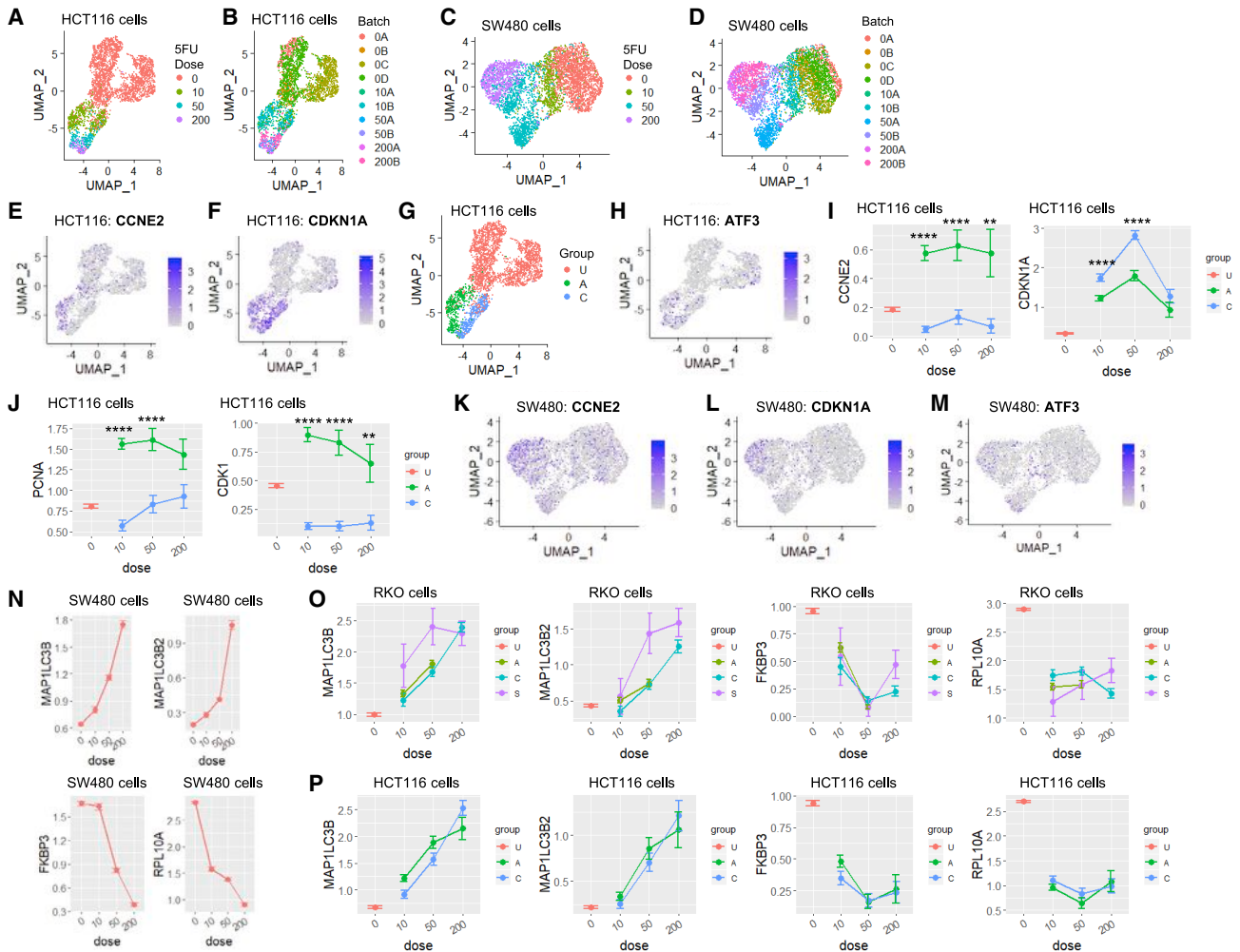


Figure 7. Conserved and Cell-Line-Specific Features of Single-Cell DNA Damage Response

(A–H and K–M) UMAP manifolds and gene expression feature plots of control and 5FU-treated HCT116 (A, B, and E–H) and SW480 (C, D, and K–M) cells. UMAP manifolds were indicated in color by 5FU treatment dose (A and C), batch (B and D), group assignment (G), or indicated gene expression (E, F, H, and K–M). (I, J, N, O, and P) Gene expression analyses (y axis) across different subgroups of cells partitioned with 5FU dose (x axis) and group identity (color). Untreated, apoptotic, and checkpoint groups of HCT116 cells (I, J, and P); untreated, apoptotic, checkpoint, and stress groups of RKO cells (O); or entire SW480 cell population (N) were analyzed. Data are presented as mean \pm SEM. **p < 0.01; ****p < 0.0001, in Sidak's multiple comparison test between apoptotic and checkpoint groups (I and J). See also Figure S7.

levels (Liu et al., 2016). In the scRNA-seq dataset, the transcriptional burst event (biological effect) and dropout event (technical effect) can further decrease this concordance (Hicks et al., 2018). Stress insults may substantially alter the steady-state levels of protein expression through transcription-independent mechanisms such as translational control or protein degradation control (Liu et al., 2016). Therefore, abundance or scarcity of mRNA species might not directly translate into changes in the corresponding protein levels.

Because our work focuses on heterogeneous DNA damage responses, we preliminarily examined the expression of CCNE2 and CDKN1A proteins, whose encoding mRNAs are among the top markers for the apoptotic and checkpoint groups, respectively. Comparative analysis of scRNA-seq and flow cytometry data indi-

cated that, at both mRNA levels and protein levels, gene products for CCNE2 and CDKN1A showed a mutually exclusive pattern of gene expression. Furthermore, in each dataset, these bipartite gene induction responses were correlated with different cell-fate responses to DNA damage, as manifested by GO analyses and cell-cycle estimation analyses (scRNA-seq data), DNA content assays, caspase activity assays, and P-H2AX level assays (flow cytometry data). Therefore, even though we cannot assume a linear correlation between mRNA and protein levels, it is likely that the expression levels of CCNE2 and CDKN1A gene products are sufficient to distinguish two different groups of cell populations undergoing distinct cell-fate responses.

In addition to transcriptional regulation, CCNE2 and CDKN1A are known to be post-transcriptionally regulated through protein

degradation. CCNE2 is degraded by an E3 ligase complex containing FBXW7 (Klotz et al., 2009), whose encoding mRNA is p53 inducible and upregulated in the apoptotic group (Figure 3B). The *FBXW7* upregulation might function in limiting the protein level of CCNE2 in this group of cells. Likewise, CDKN1A is degraded by MDM2 (Zhang et al., 2004), whose encoding mRNA is upregulated in the checkpoint group (Figure 3C), possibly limiting the CDKN1A protein expression in this group. Interestingly, CDKN1A is also degraded by a PCNA-containing protein complex (Sheng et al., 2019). Since PCNA was highly expressed in the apoptotic group (Figure S4C), PCNA may contribute to accentuating bipartite CDKN1A protein expression by further reducing CDKN1A levels in the apoptotic group of cells, which already expresses low amounts of *CDKN1A* mRNAs. Since multiple additional mechanisms can be involved in determining the expression levels of proteins, future studies should explore the single-cell proteome responses to DNA damage.

Another limitation of our scRNA-seq dataset is that it was produced with a single DNA-damaging agent, 5FU. Although 5FU is among the most frequently used genotoxic chemotherapy agents, different types of DNA damage may produce different patterns of heterogeneous DNA damage response. To address this, we tested whether camptothecin and etoposide, two genotoxic drugs that are unrelated to 5FU, can produce bipartite DNA damage responses in CCNE2 and CDKN1A expression. As observed from the 5FU experiments, both etoposide and camptothecin induced the emergence of apoptotic (CCNE2-high, CDKN1A-low) and checkpoint (CCNE2-low, CDKN1A-high) populations, which underwent corresponding cell-fate responses. Thus, these heterogeneous cell fate and gene expression patterns appear to be conserved in multiple DNA-damaging chemotherapeutic agents.

Still, it is likely that at least some of the features described in our data are specific to 5FU. 5FU is known to induce RNA damage (Longley et al., 2003), which could compromise cellular protein quality and provoke endoplasmic reticulum (ER) stress. Diverse ER-stress-responsive proteins, including *ATF3*, *XBP1*, and *DDIT3/CHOP*, were strongly induced in the stress group of cells after 5FU treatment. Thus, it is possible that some of these transcriptional features are 5FU specific. The generation of additional scRNA-seq datasets in response to different types of chemotherapeutic agents, and, most importantly, single-cell characterization of *in vivo* DNA damage responses are important future directions.

It should also be noted that our current scRNA-seq method only captures a snapshot of the transcriptome at one time point: after 24 h of 5FU treatment. The transcriptomic landscape of 5FU-treated cells is likely to change substantially over time. For instance, CDKN1A expression levels are dynamically changed with heterogeneous longitudinal patterns that can predict cell-fate consequences (Barr et al., 2017; Hsu et al., 2019; Sheng et al., 2019). Our study presented here suggests that, in addition to CDKN1A, many additional genes are differentially regulated across the groups of cells undergoing distinct fate responses. Whether and how these differential expression patterns are longitudinally maintained or altered should serve as a focus for future investigations and might be approachable using

recently developed techniques monitoring single-cell gene expression dynamics (Cao et al., 2020; Erhard et al., 2019). These experiments should be performed at multiple time points to comprehensively understand how the single-cell transcriptome landscape changes over time after 5FU treatment.

Tumor suppressor p53 is an important DNA-damage-regulated transcription factor that is responsible for the regulation of many genes that are group specifically expressed. Through several elegant studies, it was shown that transient pulses of p53 activation can produce cell-cycle arrest, while a sustained activation can lead to apoptosis (Hafner et al., 2019; Purvis and Lahav, 2013). Based on those earlier studies, we speculate that, in our experiments, the apoptotic group cells underwent prolonged p53 activation, while the checkpoint group cells produced transient pulses of p53 activation. This hypothesis is consistent with our observation that the ISG15-mediated positive-feedback loop, which can produce sustained p53 activation (Park et al., 2016), was more prominent in the apoptotic group, while the MDM2-mediated negative-feedback loop, which is critical for producing pulse responses (Batchelor et al., 2009), was more prominent in the checkpoint and stress groups. The potential role of p53 in producing heterogeneous transcriptome responses is also consistent with our observation that single-cell transcriptome heterogeneity in the DNA damage response is more pronounced in p53-proficient RKO and HCT116 cells than in p53-mutated SW480 cells. In the future, technologies such as single-cell ChIP-seq (Grosselin et al., 2019) could be used to further characterize the heterogeneous p53 responses across cells undergoing different fates. Mechanistic studies using gene knockouts or mutations should also be performed to clarify the role of p53 in heterogeneous transcriptome responses after DNA damage.

In summary, our work provides a snapshot of how individual cells shape their transcriptome in response to DNA damage. This work unveils information about how single-cell gene expression patterns are diversified across different subgroups undergoing distinct cell fates. By revealing cell-fate-specific transcriptome patterns, we open an avenue for future studies to further explore heterogeneous cancer cell responses to genotoxic chemotherapy, such as fractional killing and chemoresistant tumor recurrence.

STAR★METHODS

Detailed methods are provided in the online version of this paper and include the following:

- KEY RESOURCES TABLE
- RESOURCE AVAILABILITY
 - Lead Contact
 - Materials Availability
 - Data and Code Availability
- EXPERIMENTAL MODEL AND SUBJECT DETAILS
- METHOD DETAILS
 - DNA damage treatment
 - Drop-seq and library preparation
 - Flow cytometry
 - Immunoblotting

- Quantitative RT-PCR
- **QUANTIFICATION AND STATISTICAL ANALYSIS**
 - Drop-seq data processing and cell line de-multiplexing
 - Cell clustering and data visualization
 - Pathway enrichment analysis
 - Imputation of single cell expression

SUPPLEMENTAL INFORMATION

Supplemental Information can be found online at <https://doi.org/10.1016/j.celrep.2020.108077>.

ACKNOWLEDGMENTS

We thank Dr. Y. Shah for cell lines; B. Gu, I.A. Semple, and B. Kim for technical assistance; Santa Cruz Biotechnology for antibodies; and Drs. M. Kim, Y. Xi, J. Connett, A.H. Kowalsky, and K.R. Spindler for their intellectual input and editorial assistance. This work was supported by the NIH (R01DK102850 and R01DK114131 to J.H.L., U01HL137182 to H.M.K., and P30AG024824, P30DK034933, P30DK089503, and P30CA046592), the Chan Zuckerberg Initiative (to H.M.K.), the MCubed Initiative (to J.H.L., H.M.K., and C.H.K.), the Organogenesis Fellowship (to S.N.), and an American Association for the Study of Liver Diseases pilot research award (to J.H.L. and H.M.K.).

AUTHOR CONTRIBUTIONS

S.R.P. performed all experiments. S.N., Y.-C.C., E.Y., and H.K. helped with Drop-seq. L.F. and C.-S.C. helped with experiments. Z.Z.Z. helped with statistical analysis. L.F. and C.H.K. helped with flow cytometry. H.M.K. and J.H.L. conceived and directed the project. S.R.P., H.M.K., and J.H.L. designed experiments, analyzed data, and wrote the manuscript. All authors revised or commented on the manuscript and approved the final version.

DECLARATION OF INTERESTS

The authors declare no competing interests.

Received: November 6, 2019

Revised: May 4, 2020

Accepted: August 5, 2020

Published: August 25, 2020

REFERENCES

Ahmed, D., Eide, P.W., Eilertsen, I.A., Danielsen, S.A., Eknæs, M., Hektoen, M., Lind, G.E., and Lothe, R.A. (2013). Epigenetic and genetic features of 24 colon cancer cell lines. *Oncogenesis* 2, e71.

Auton, A., Brooks, L.D., Durbin, R.M., Garrison, E.P., Kang, H.M., Korbel, J.O., Marchini, J.L., McCarthy, S., McVean, G.A., and Abecasis, G.R.; 1000 Genomes Project Consortium (2015). A global reference for human genetic variation. *Nature* 526, 68–74.

Barr, A.R., Cooper, S., Heldt, F.S., Butera, F., Stoy, H., Mansfeld, J., Novák, B., and Bakal, C. (2017). DNA damage during S-phase mediates the proliferation-quiescence decision in the subsequent G1 via p21 expression. *Nat. Commun.* 8, 14728.

Batchelor, E., Loewer, A., and Lahav, G. (2009). The ups and downs of p53: understanding protein dynamics in single cells. *Nat. Rev. Cancer* 9, 371–377.

Becht, E., McInnes, L., Healy, J., Dutertre, C.-A., Kwok, I.W.H., Ng, L.G., Ginhoux, F., and Newell, E.W. (2018). Dimensionality reduction for visualizing single-cell data using UMAP. *Nat. Biotechnol.* 37, 38–44.

Bunz, F., Hwang, P.M., Torrance, C., Waldman, T., Zhang, Y., Dillehay, L., Williams, J., Lengauer, C., Kinzler, K.W., and Vogelstein, B. (1999). Disruption of p53 in human cancer cells alters the responses to therapeutic agents. *J. Clin. Invest.* 104, 263–269.

Butler, A., Hoffman, P., Smibert, P., Papalexi, E., and Satija, R. (2018). Integrating single-cell transcriptomic data across different conditions, technologies, and species. *Nat. Biotechnol.* 36, 411–420.

Cao, J., Zhou, W., Steemers, F., Trapnell, C., and Shendure, J. (2020). Sci-fate characterizes the dynamics of gene expression in single cells. *Nat. Biotechnol.* 38, 980–988.

Chang, G.S., Chen, X.A., Park, B., Rhee, H.S., Li, P., Han, K.H., Mishra, T., Chan-Salis, K.Y., Li, Y., Hardison, R.C., et al. (2014). A comprehensive and high-resolution genome-wide response of p53 to stress. *Cell Rep.* 8, 514–527.

Darzynkiewicz, Z., Juan, G., Li, X., Gorczyca, W., Murakami, T., and Traganos, F. (1997). Cytometry in cell necrobiology: analysis of apoptosis and accidental cell death (necrosis). *Cytometry* 27, 1–20.

Dobin, A., Davis, C.A., Schlesinger, F., Drenkow, J., Zaleski, C., Jha, S., Batut, P., Chaisson, M., and Gingeras, T.R. (2013). STAR: ultrafast universal RNA-seq aligner. *Bioinformatics* 29, 15–21.

Enari, M., Sakahira, H., Yokoyama, H., Okawa, K., Iwamoto, A., and Nagata, S. (1998). A caspase-activated DNase that degrades DNA during apoptosis, and its inhibitor ICAD. *Nature* 391, 43–50.

Erhard, F., Baptista, M.A.P., Krammer, T., Hennig, T., Lange, M., Arampatzis, P., Jürges, C.S., Theis, F.J., Saliba, A.E., and Dölken, L. (2019). scSLAM-seq reveals core features of transcription dynamics in single cells. *Nature* 571, 419–423.

Fischer, M. (2017). Census and evaluation of p53 target genes. *Oncogene* 36, 3943–3956.

Gene Ontology Consortium (2015). Gene Ontology Consortium: going forward. *Nucleic Acids Res.* 43, D1049–D1056.

Grosselin, K., Durand, A., Marsolier, J., Poitou, A., Marangoni, E., Nemati, F., Dahmani, A., Lameiras, S., Reyat, F., Frenoy, O., et al. (2019). High-throughput single-cell ChIP-seq identifies heterogeneity of chromatin states in breast cancer. *Nat. Genet.* 51, 1060–1066.

Hafner, A., Bulyk, M.L., Jambhekar, A., and Lahav, G. (2019). The multiple mechanisms that regulate p53 activity and cell fate. *Nat. Rev. Mol. Cell Biol.* 20, 199–210.

Haghverdi, L., Lun, A.T.L., Morgan, M.D., and Marioni, J.C. (2018). Batch effects in single-cell RNA-sequencing data are corrected by matching mutual nearest neighbors. *Nat. Biotechnol.* 36, 421–427.

Harper, J.W., and Elledge, S.J. (2007). The DNA damage response: ten years after. *Mol. Cell* 28, 739–745.

Hicks, S.C., Townes, F.W., Teng, M., and Irizarry, R.A. (2018). Missing data and technical variability in single-cell RNA-sequencing experiments. *Biostatistics* 19, 562–578.

Ho, A., Cho, C.S., Namkoong, S., Cho, U.S., and Lee, J.H. (2016). Biochemical Basis of Sestrin Physiological Activities. *Trends Biochem. Sci.* 41, 621–632.

Hsu, C.H., Altschuler, S.J., and Wu, L.F. (2019). Patterns of Early p21 Dynamics Determine Proliferation-Senescence Cell Fate after Chemotherapy. *Cell* 178, 361–373.e12.

Jackson, S.P., and Bartek, J. (2009). The DNA-damage response in human biology and disease. *Nature* 461, 1071–1078.

Kanehisa, M., and Goto, S. (2000). KEGG: kyoto encyclopedia of genes and genomes. *Nucleic Acids Res.* 28, 27–30.

Kang, H.M., Subramaniam, M., Targ, S., Nguyen, M., Maliskova, L., McCarthy, E., Wan, E., Wong, S., Byrnes, L., Lanata, C.M., et al. (2018). Multiplexed droplet single-cell RNA-sequencing using natural genetic variation. *Nat. Biotechnol.* 36, 89–94.

Kho, P.S., Wang, Z., Zhuang, L., Li, Y., Chew, J.L., Ng, H.H., Liu, E.T., and Yu, Q. (2004). p53-regulated transcriptional program associated with genotoxic stress-induced apoptosis. *J. Biol. Chem.* 279, 21183–21192.

Klotz, K., Cepeda, D., Tan, Y., Sun, D., Sangfelt, O., and Spruck, C. (2009). SCF(Fbxw7/hCdc4) targets cyclin E2 for ubiquitin-dependent proteolysis. *Exp. Cell Res.* 315, 1832–1839.

Knight, K. (2018). Intracellular Flow Cytometry Staining Protocol. <https://www.protocols.io/view/intracellular-flow-cytometry-staining-protocol-tknekve>.